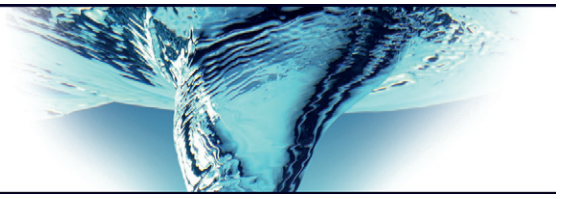
*J. Fluid Mech.* (2016), *vol.* 790, R3, doi:10.1017/jfm.2016.55



JFM RAPIDS
journals.cambridge.org/rapids

# Thermal convection in inclined cylindrical containers

**Olga Shishkina**[1,†] **and Susanne Horn**[2]

[1]Max Planck Institute for Dynamics and Self-Organization, Am Fassberg 17, 37077 Göttingen, Germany

[2]Department of Mathematics, Imperial College London, London SW7 2AZ, UK

(Received 12 December 2015; revised 13 January 2016; accepted 14 January 2016; first published online 11 February 2016)

By means of direct numerical simulations (DNS) we investigate the effect of a tilt angle $\beta$, $0 \leqslant \beta \leqslant \pi/2$, of a Rayleigh–Bénard convection (RBC) cell of aspect ratio 1, on the Nusselt number $Nu$ and Reynolds number $Re$. The considered Rayleigh numbers $Ra$ range from $10^6$ to $10^8$, the Prandtl numbers range from 0.1 to 100 and the total number of the studied cases is 108. We show that the $Nu\,(\beta)/Nu(0)$ dependence is not universal and is strongly influenced by a combination of $Ra$ and $Pr$. Thus, with a small inclination $\beta$ of the RBC cell, the Nusselt number can decrease or increase, compared to that in the RBC case, for large and small $Pr$, respectively. A slight cell tilt may not only stabilize the plane of the large-scale circulation (LSC) but can also enforce an LSC for cases when the preferred state in the perfect RBC case is not an LSC but a more complicated multiple-roll state. Close to $\beta = \pi/2$, $Nu$ and $Re$ decrease with increasing $\beta$ in all considered cases. Generally, the $Nu(\beta)/Nu(0)$ dependence is a complicated, non-monotonic function of $\beta$.

**Key words:** Bénard convection, convection, convection in cavities

## 1. Introduction

Fluid motion driven by an imposed temperature gradient is a common phenomenon in nature and is important in many industrial applications. In the classical models of thermal convection, i.e. Rayleigh–Bénard convection (RBC) and vertical convection (VC), the fluid is confined between a heated plate and a cooled plate which are parallel to each other. The induced flow is determined by the Rayleigh number $Ra \equiv \alpha g \Delta H^3/(\kappa \nu)$, Prandtl number $Pr \equiv \nu/\kappa$ and the aspect ratio of the container $\Gamma \equiv D/H$. Here $\alpha$ denotes the isobaric thermal expansion coefficient, $\nu$ the kinematic viscosity, $\kappa$ the thermal diffusivity of the fluid, $g$ the acceleration due to gravity, and

† Email address for correspondence: Olga.Shishkina@ds.mpg.de

© Cambridge University Press 2016



https://doi.org/10.1017/jfm.2016.55 Published online by Cambridge University Press

$\Delta \equiv T_+ - T_-$ the temperature difference between the warm ($T_+$) and the cold ($T_-$) isothermal boundaries. We will only consider cylindrical vessels, characterized by the diameter $D$ and the distance $H$ between the heated and cooled plates.

The essential difference between RBC and VC is the direction of the gravity vector, i.e. it is parallel to the isothermal surfaces of the container in the case of VC and perpendicular to them in RBC. However, the respective flows are different and the Reynolds number $Re$ and the mean heat flux, described by the Nusselt number $Nu$, exhibit very different dependences on $Ra$ and $Pr$. For reviews on these two classical convection models, we refer to Castaing *et al.* (1989), Siggia (1994), Bodenschatz, Pesch & Ahlers (2000), Ahlers, Grossmann & Lohse (2009), Lohse & Xia (2010), Chillà & Schumacher (2012) and Ng *et al.* (2015), respectively.

Experimental studies of turbulent thermal convection in long cylinders filled with low-Prandtl-number fluids show that the most effective convective heat transfer between the heated and cooled parallel surfaces of the container occurs neither in a standing position of the cylinder (as in RBC, with a cell inclination angle $\beta = 0$), nor in a lying position (as in VC, $\beta = 0.5\pi$), but in an inclined container, for a certain intermediate value of $\beta$, $0 < \beta < 0.5\pi$. Such measurements in liquid sodium, $Pr \sim 0.01$, are reported by Frick *et al.* (2015), Kolesnichenko *et al.* (2015) and Vasilev *et al.* (2015). Moreover, these experiments show that, in the case of small $Pr$ ($Pr \ll 1$) and relatively large $Ra$ ($Ra \gtrsim 10^9$), any tilt $\beta$, $0 < \beta \leqslant \pi/2$, of the cell leads to an increase of $Nu$, compared to that in the RBC case ($\beta = 0$). Langebach & Haberstroh (2014) also obtained similar results in their experimental study for $Pr \approx 0.7$.

The effect of the cell tilting on convective heat transport in large-Prandtl-number fluids is very different from that in the case of low-Prandtl-number fluids. Thus, experiments by Guo *et al.* (2015) in a parallelepiped container for $Pr \approx 6.7$ and $Ra \approx 4.4 \times 10^9$ showed a monotonic reduction of $Nu$ with increasing $\beta$ for $\beta \in [0, \pi/2]$.

One should note that most of the investigations of the effects of cell tilt on the mean heat transport were conducted in a narrow region of $\beta$ close to 0, and mainly for $Pr > 1$. These studies generally show a small effect of the cell inclination on the mean heat transport (Ciliberto, Cioni & Laroche 1996; Cioni, Ciliberto & Sommeria 1997; Ahlers, Brown & Nikolaenko 2006; Roche *et al.* 2010; Wei & Xia 2013). Measurements by Chillà *et al.* (2004) for $0 < \beta \lesssim 0.01\pi$ and $5 \times 10^{11} \leqslant Ra \leqslant 4 \times 10^{12}$ in a cylindrical container of $\Gamma = 1/2$, filled with hot water, $Pr \approx 2$, showed a reduction of the normalized Nusselt number $Nu(\beta)/Nu(0)$ approximately as $1–2\beta$, if a two-roll global flow structure developed. For $Pr \approx 4.3$ and $3 \times 10^9 \lesssim Ra \lesssim 7 \times 10^{10}$ Sun, Xi & Xia (2005) also found a reduction of $Nu$ if their cylindrical ($\Gamma = 1/2$) RBC cell was tilted by $\beta \approx 0.01\pi$. As the reduction in $Nu$ with cell tilt was associated with the development of a two-roll flow structure, no significant reduction in $Nu$ was expected in a slightly inclined cell with $\Gamma = 1$. Measurements by Ahlers *et al.* (2006) in a $\Gamma = 1$ cylindrical cell filled with water ($Pr \approx 4.3$) for Rayleigh numbers of approximately $10^{11}$ indeed showed only a tiny reduction of $Nu$, namely as $Nu(\beta)/Nu(0) \approx 1 - 0.03\beta$, and a much stronger Reynolds-number dependence $Re(\beta)/Re(0) \approx 1 + 1.85\beta - 5.9\beta^2$. For similar $Pr$, $\Gamma = 1/2$ and $Ra = 1.8 \times 10^{10}$ and $7.2 \times 10^{10}$, Weiss & Ahlers (2013) even found a very small increase of the mean heat transport with a local maximum at $\beta \approx 0.02\pi$. This increase was explained by a stabilization of the single-roll state of the large-scale circulation (LSC) and a destabilization of the double-roll state, which are associated with, respectively, an increase and decrease of the mean heat transport. From all these experimental results one can already conclude that the $Nu(\beta)/Nu(0)$ dependence near $\beta = 0$ depends strongly on $Ra$, $Pr$ and $\Gamma$, and is a complicated



https://doi.org/10.1017/jfm.2016.55 Published online by Cambridge University Press

function of these parameters, which cannot be represented as a simple product of their power functions.

In the present study, we investigate the effect of a cell tilt, reflected in the inclination angle $\beta$, $0 \leqslant \beta \leqslant \pi/2$, on the Nusselt and Reynolds numbers by means of direct numerical simulations (DNS) of thermal convection in a cylindrical vessel with aspect ratio 1.

## 2. Results

The following combinations of $Ra$ and $Pr$ were considered in our three-dimensional DNS: $Ra = 10^6$ for $Pr = 0.1$, 1, 10 and 100; $Ra = 10^7$ for $Pr = 1$ and 10; and $Ra = 10^8$ for $Pr = 1$. For each combination of $Ra$ and $Pr$ we studied thermal convection under the Oberbeck–Boussinesq approximation, in inclined cylindrical containers with $\Gamma = 1$ and with different inclination angles $\beta$ that varied between 0 (RBC) and $\pi/2$ (VC). Thus, the problem is governed by the Navier–Stokes equations in cylindrical coordinates $(r, \phi, z)$:

$$\boldsymbol{\nabla} \cdot \boldsymbol{u} = 0, \tag{2.1}$$

$$D_t \boldsymbol{u} = \nu \nabla^2 \boldsymbol{u} - \boldsymbol{\nabla} p + \alpha g (T - T_0) \hat{\boldsymbol{e}}, \tag{2.2}$$

$$D_t T = \kappa \nabla^2 T, \tag{2.3}$$

where $D_t$ denotes the substantial derivative, $\boldsymbol{u} = (u_r, u_\phi, u_z)$ the velocity vector, $p$ the reduced kinetic pressure, $T$ the temperature, $T_0 = (T_+ + T_-)/2$ and $\hat{\boldsymbol{e}}$ is the unit vector, $\hat{\boldsymbol{e}} = (-\sin(\beta)\cos(\phi), \sin(\beta)\sin(\phi), \cos(\beta))$. These equations are non-dimensionalized by using the cylinder radius $R$ and the quantities $(\alpha g R \Delta)^{1/2}$, $R(\alpha g R \Delta)^{-1/2}$ and $\Delta$ as units of length, velocity, time and temperature, respectively. (Note that in the definition of $Ra$, not the cylinder radius $R$, but the cylinder height $H$ is used as the reference length.)

The resulting dimensionless equations are solved numerically with the code GOLDFISH, as in Shishkina *et al.* (2015) and Shishkina & Wagner (2016). Computational grids of up to $(N_r, N_\phi, N_z) = (192, 512, 384)$ nodes satisfy the resolution requirements for DNS (Shishkina *et al.* 2010).

The stepping in the $\beta$-range varies from $0.0025\pi$ to $0.05\pi$, with a minimum of 11 and a maximum of 22 different inclination angles between 0 (RBC) and $\pi/2$ (VC). The refined $\beta$-resolution is applied for cases that are near $\beta = 0$. This helps to better understand the behaviour of $Nu$ and $Re$ in inclined convection close to the exact RBC case, which is particularly relevant for experimental set-ups. In total, we studied 108 different combinations of $Ra$, $Pr$ and $\beta$.

In figure 1 isosurfaces of the instantaneous temperature are presented for $Pr = 1$ and $Ra = 10^6$, $10^7$ and $10^8$, and six particular inclination angles $\beta = 0$ (RBC), $0.1\pi$, $0.2\pi$, $0.3\pi$, $0.4\pi$ and $0.5\pi$ (VC). In the RBC set-up ($\beta = 0$) the flows are always unsteady or even turbulent and, due to the aspect ratio of $\Gamma = 1$ and relatively small $Pr$, the global flow structure is a large-scale circulation (LSC) filling the whole cell. However, the orientation of the LSC is not fixed and changes with time (e.g. Brown & Ahlers 2006).

With a small inclination $\beta$, the LSC is fixed to the inclination plane, and likewise is its rotation direction. The flow is reorganized in such a way that fluid near the heated (cooled) plate ascends (descends) closer to the sidewall; hence, most of the interior fluid is almost quiescent and has a mean temperature of approximately $T = (T_+ + T_-)/2$. For $\beta \gtrsim 0.3\pi$ the interior temperature field shows signs of stratification,



https://doi.org/10.1017/jfm.2016.55 Published online by Cambridge University Press

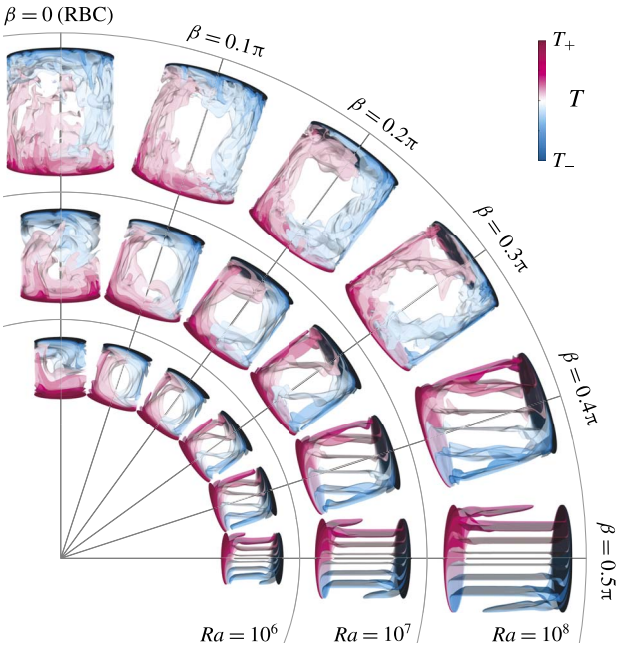



FIGURE 1. Isosurfaces of the instantaneous temperature fields in inclined convection in cylindrical containers filled with a fluid of $Pr = 1$, for $Ra = 10^6$, $10^7$ and $10^8$, and different inclination angles $\beta = 0$, $0.1\pi$, $0.2\pi$, $0.3\pi$, $0.4\pi$ and $0.5\pi$, as obtained in our DNS. Shown are ten isosurfaces that are equidistantly distributed between the heated ($T_+$) and cooled ($T_-$) cell boundaries. The proportions between the different sizes of the presented convection cells reflect the proportions between the different $Ra$.

i.e. the temperature isosurfaces align horizontally. Further, with increasing $\beta$ the corner rolls are less pronounced (if they exist) and the flow generally stabilizes. Thus, we observe steady flows for $Ra = 10^6$ if $\beta \gtrsim 0.2\pi$, for $Ra = 10^7$ if $\beta \gtrsim 0.3\pi$, and even for $Ra = 10^8$ if $\beta \gtrsim 0.45\pi$. However, with increasing $Ra$ and $\beta = 0.5\pi$ (VC) the up-flow and down-flow along the isothermal plates becomes more vigorous, and the flow impinging on the viscous boundary layer adjacent to the adiabatic wall leads to distinct overshooting in the temperature, and ultimately to a rolling up of the fluid and consequent instability.

Furthermore, we conducted DNS for $Pr = 0.1$, 1, 10 and 100 for a fixed $Ra = 10^6$ (see figure 2) to investigate how the cell tilt influences convection in fluids with different $Pr$. For $\beta = 0$ the LSC develops in a singe large-roll state if $Pr$ is small, while for large $Pr$ ($Pr = 100$) a more complicated global flow structure develops (Horn, Shishkina & Wagner 2013; Horn & Shishkina 2014). With a tiny inclination angle $\beta$, the flow is reorganized in a one-roll LSC even if $Pr$ is large. Thus, for $Pr = 100$, we observe this already for $\beta = 0.005\pi (= 0.9°)$, see figure 3. Again, all flows are stabilized with increasing $\beta$. For $Ra = 10^6$, $\Gamma = 1$, $\beta = 0$ and all considered $Pr$ the flows are unsteady, but already for $\beta \gtrsim 0.06\pi$ ($Pr = 100$), $\beta \gtrsim 0.15\pi$ ($Pr = 10$), $\beta \gtrsim 0.2\pi$ ($Pr = 1$) and $\beta \gtrsim 0.4\pi$ ($Pr = 0.1$) steady convective flows are observed.

Quantitative characteristics of the inclined convection flows, i.e. the Nusselt number,

$$Nu(z) \equiv (\langle u_z T\rangle_z - \kappa \partial_z \langle T\rangle_z)/(\kappa \Delta/H) = \text{const.}, \tag{2.4}$$



https://doi.org/10.1017/jfm.2016.55 Published online by Cambridge University Press

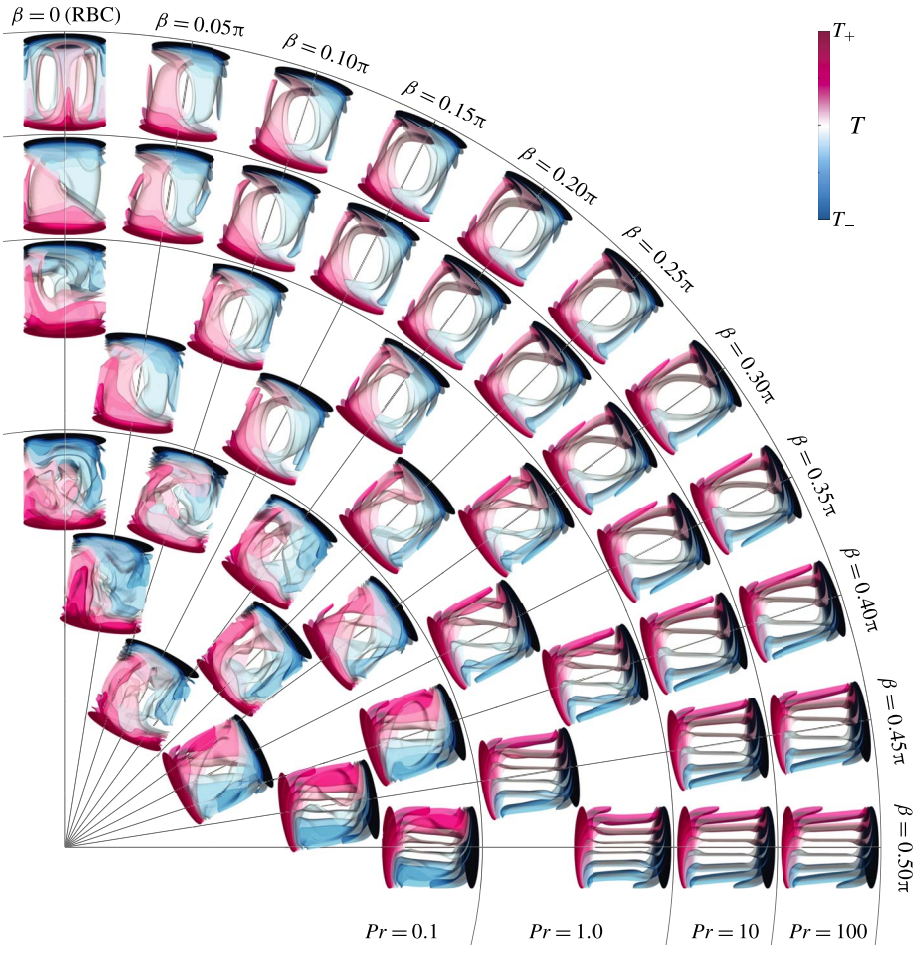



FIGURE 2. Isosurfaces of the instantaneous temperature fields in inclined convection in cylindrical containers, filled with a fluid of $Pr = 0.1$, $Pr = 1$, $Pr = 10$ or $Pr = 100$, for $Ra = 10^6$ and different inclination angles from $\beta = 0$ to $\beta = 0.5\pi$, as obtained in our DNS. Shown are ten isosurfaces that are equidistantly distributed between the heated ($T_+$) and cooled ($T_-$) cell boundaries.

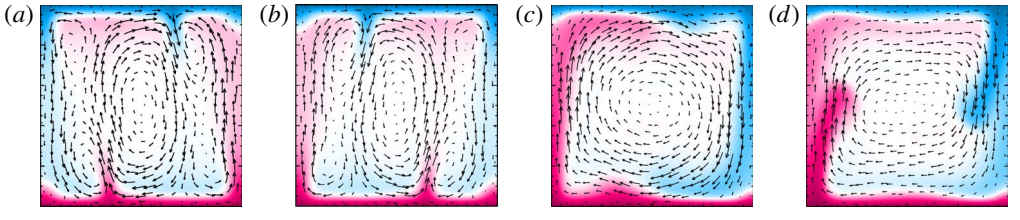



FIGURE 3. Changing of the instantaneous temperature fields with a small inclination angle $\beta$ for $Pr = 100$ and $Ra = 10^6$. Colour scale as in figure 2. (*a*) $\beta = 0$, (*b*) $0.0025\pi$, (*c*) $0.0050\pi$, (*d*) $0.0075\pi$.

https://doi.org/10.1017/jfm.2016.55 Published online by Cambridge University Press

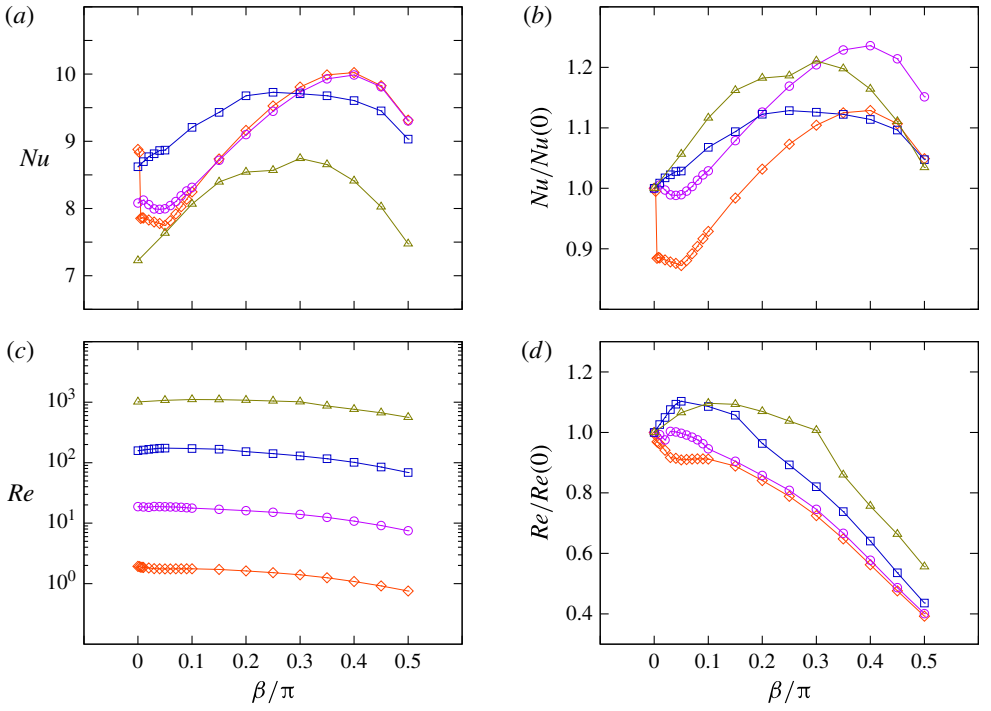



FIGURE 4. Absolute and normalized Nusselt and Reynolds numbers in inclined convection in a cylinder of aspect ratio 1, for $Ra = 10^6$ and $Pr = 0.1$ (triangles), $Pr = 1$ (squares), $Pr = 10$ (circles) and $Pr = 100$ (diamonds), as functions of the inclination angle $\beta$. (*a*) Absolute Nusselt numbers $Nu$. (*b*) Normalized Nusselt numbers $Nu/Nu(0)$. (*c*) Absolute Reynolds numbers $Re$. (*d*) Normalized Reynolds numbers $Re/Re(0)$. Normalization was carried out using the corresponding values for RBC ($\beta = 0$).

and the Reynolds number,

$$Re \equiv \sqrt{\langle \boldsymbol{u} \cdot \boldsymbol{u} \rangle} H/\nu \tag{2.5}$$

for different $Pr$ are presented in figure 4. Here, $\langle \cdot \rangle_z$ denotes the temporal and planar average at distance $z$ from the heated plate and $\langle \cdot \rangle$ denotes the average in time and over the whole convection cell.

The curves of $Nu(\beta)$ for small $Pr$ ($Pr = 1$ and $Pr = 0.1$) and large $Pr$ ($Pr = 10$ and $Pr = 100$) look very different (see figure 4*a*). In the small-$Pr$ case, $Nu$ increases with any small tilt of a RBC ($\beta = 0$) or VC ($\beta = \pi/2$) cell. The global maximum of $Nu$ is obtained for an intermediate value of $\beta$. The absolute values of $Nu$ are smaller for smaller $Pr$ (figure 4*a*), but the relative increase of the mean heat transport $Nu(\beta)/Nu(0)$ is larger for smaller $Pr$ (figure 4*b*).

The curves of $Nu(\beta)$ for large $Pr$ ($Pr = 10$ and $Pr = 100$) almost replicate each other for $\beta \geqslant 0.1\pi$ and differ only near $\beta = 0$. With a small tilt of the RBC cell ($\beta$ close to 0) a tiny increase of $Nu$ is possible. This effect is similar to that found by Weiss & Ahlers (2013) in their measurements in water. With further inclination of the cell, the $Nu(\beta)$ curve turns down; this drop of the Nusselt number is more pronounced for larger $Pr$. For $Ra = 10^6$, already by $\beta \approx 0.05\pi$ the value of $Nu(\beta)$ starts to increase until $\beta \approx 0.4\pi$, where it reaches its global maximum, and after that it decreases with increasing $\beta$ until $\beta = \pi/2$.



https://doi.org/10.1017/jfm.2016.55 Published online by Cambridge University Press

The Reynolds numbers are presented in figure 4(*c*,*d*). On a log-scale the general behaviour of $Re$ seems similar for all $Pr$; however, the normalized Reynolds numbers, $Re(\beta)/Re(0)$, reveal a very different dependence on the cell tilt, especially for small $\beta$. Remarkably, for $Pr = 0.1$ and 1 the Reynolds number increases, while for $Pr = 100$ it decreases, and for $Pr = 10$, $Re(\beta)/Re(0)$ drops, increases, and then drops again.

Both curves for $Pr = 10$ and for $Pr = 100$ show a couple of kinks which can be related to the different preferred large-scale flow states, which can be steady or oscillatory. For $Pr = 1$ the initial increase with $\beta$ is related to unsteady convection and a sufficiently efficient buoyancy-induced mixing of the bulk. For larger tilt angles, $0.05\pi \lesssim \beta \lesssim 0.15\pi$, the flow stabilizes, and an oscillating LSC develops that is reflected in the slow decrease in $Re$. Finally, for completely steady convection at $\beta \gtrsim 0.15$, $Re(\beta)/Re(0)$ decreases, but now much more sharply. Similarly, for $Pr = 0.1$, the initial increase up to $\beta \approx 0.15\pi$ is due to the unsteady mixing in the bulk. The competing effect of stratification caused by the inclination then leads first to a gentle down-slope. Eventually, for $\beta \gtrsim 0.3\pi$, the flow becomes steady and $Re(\beta)/Re(0)$ drops abruptly. Hence, in all cases $Re(\beta)/Re(0)$ decreases with increasing $\beta$ near $\beta = \pi/2$ (VC state) with a similar slope. This decrease is only slightly steeper for larger $Pr$.

The Rayleigh number is evidently the other important control parameter besides $Pr$ influencing the $Nu$- and $Re$-dependences on inclined thermal convection. Thus, we conducted DNS for $Pr = 1$ where we varied $Ra$ from $10^6$ to $10^8$, and DNS for $Pr = 10$ with $Ra = 10^6$ and $10^7$. The results are shown in figure 5.

As expected, for almost all considered $Ra$, $Nu(\beta)/Nu(0)$ increases near $\beta = 0$ and decreases near $\beta = \pi/2$, see figure 5(*a*,*b*). Otherwise, the curves do not show a very distinct or apparent regularity-dependent on $Ra$. The principal structure of the $Nu(\beta)/Nu(0)$-profiles (figure 5*b*) is determined mainly by $Pr$. For $Pr = 1$, the function $Nu(\beta)/Nu(0)$ has one maximum for $Ra = 10^6$ and at least two maxima and one minimum for $Ra = 10^7$ and $Ra = 10^8$. The first maxima for $Ra = 10^7$ and $10^8$ are at approximately the same $\beta$. However, the heat transfer is most efficient at an inclination of $\beta = 0.25\pi$ for $Ra = 10^6$ and $Ra = 10^8$, but closer to the RBC case at $\beta = 0.1\pi$ for $Ra = 10^7$.

A $Pr = 10$ fluid behaves differently. In both studied cases, for $Ra = 10^6$ and $Ra = 10^7$, the heat transport is most efficient for $\beta = 0.4\pi$, i.e. closer to VC. For $Ra = 10^7$ there is another pronounced maximum at $\beta = 0.05$, albeit lower in magnitude. In contrast, for $Ra = 10^6$, the $Nu(\beta)/Nu(0)$ curve has a minimum at the very same $\beta$. For $Ra = 10^6$ only an almost negligible heat flux intensification can be found for small tilt angles, at the tiny angle of $\beta = 0.005\pi$.

For all Prandtl numbers considered, the Nusselt number in the VC case becomes gradually smaller relative to the RBC case, with increasing $Ra$; and for $Ra = 10^8$ and $Pr = 1$ it even drops below it. But neither VC nor RBC seem to be clearly distinguished states in terms of the heat transport.

The Reynolds number, on the other hand, at least for $\beta \gtrsim 0.25\pi$, shows a much more regular dependence on $\beta$, see figure 5(*c*,*d*). For all cases, the relative Reynolds number $Re(\beta)/Re(0)$ was found to decrease near $\beta = \pi/2$, and more strongly for larger $Ra$. Again, the largest variation of $Re(\beta)/Re(0)$ is found near $\beta = 0$: first it increases with $\beta$ near $\beta = 0$; then, after its maximum which is achieved within the inclination interval $[0; 0.1\pi]$, it gradually decreases.

In an attempt to gain some further insight into the complicated $Nu(\beta)$ and $Re(\beta)$ behaviour, we studied the friction velocity $u_\tau$ at the bottom plate, evaluated as

$$u_\tau^2 = \nu \partial_z \left( \langle u_r^2 + u_\phi^2 \rangle_{z=0} \right)^{1/2} \tag{2.6}$$



https://doi.org/10.1017/jfm.2016.55 Published online by Cambridge University Press

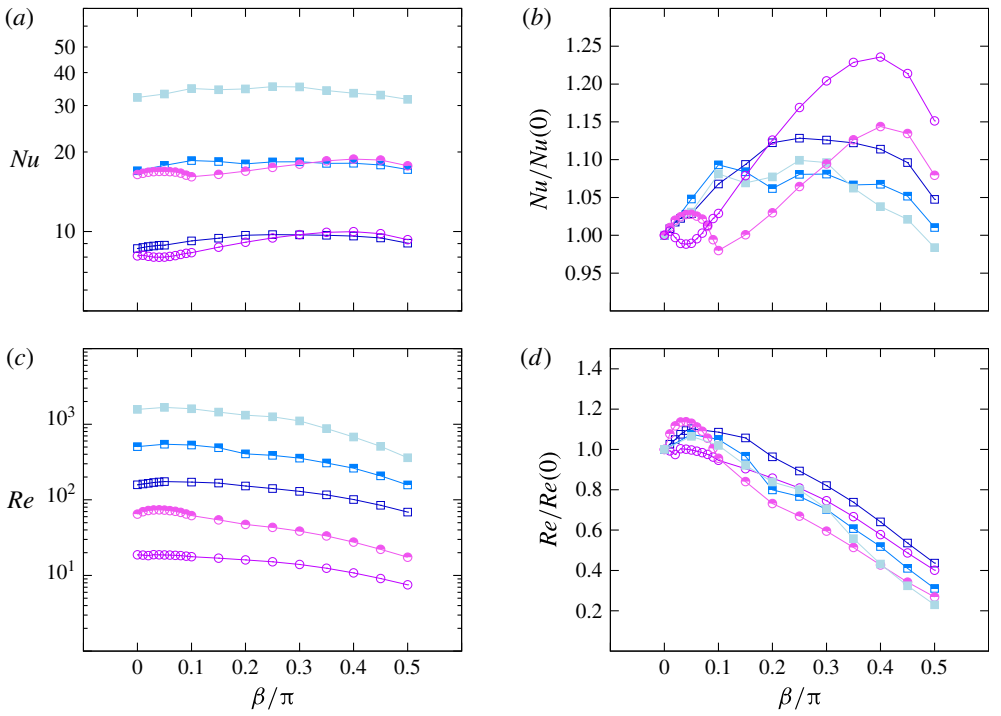



FIGURE 5. Absolute and normalized Nusselt and Reynolds numbers in inclined convection in a cylinder of aspect ratio 1, for $Pr = 1$ (squares) and $Pr = 10$ (circles), and $Ra = 10^6$ (open symbols), $Ra = 10^7$ (half filled symbols) and $Ra = 10^8$ (filled symbols), as functions of the inclination angle $\beta$. (*a*) Absolute Nusselt numbers $Nu$. (*b*) Normalized Nusselt numbers $Nu/Nu(0)$. (*c*) Absolute Reynolds numbers $Re$. (*d*) Normalized Reynolds numbers $Re/Re(0)$. Normalization was carried out using the corresponding values for RBC ($\beta = 0$).

and presented in figure 6(*a*). Contrary to the naive assumption that it should be highest for VC, since in this case the core of the fluid is stably stratified and the flow along the boundaries is a developed shear flow, the friction velocity is maximal for $\beta = 0.4\pi$. Indeed, the maximum shear velocity $u_\tau$ coincides with the maximum of $Nu$ for large $Pr$. Very likely it also contributes to the intensification of $Nu$ with decreasing $\beta$ compared to the VC case for all $Pr$. But it is not the only mechanism, and certainly not the dominant one for smaller $Pr$ and higher $Ra$. Here, the buoyancy-induced mixing and the more efficient transport by plumes along the cylinder sidewall, in particular for smaller $\beta$, seem predominantly to determine the behaviour of $Nu$ and $Re$ with $\beta$.

Finally, we evaluate the time- and volume-averaged kinetic dissipation rate $\epsilon_u = \langle \nu \sum_i (\nabla u_i)^2 \rangle$. In the particular case of $\beta = 0$ (RBC) the following exact relation holds: $\epsilon_u = (\nu^3/H^4) Pr^{-2} Ra (Nu - 1)$. With increasing but still small inclination angle $\beta$, the normalized kinetic dissipation rate $(H^4/\nu^3) Pr^2 Ra^{-1} (Nu - 1)^{-1} \epsilon_u$ might slightly increase, but already for $\beta \geqslant 0.1\pi$ it gradually decreases with increasing $\beta$ in all studied cases. The $\beta$-dependences of the normalized $\epsilon_u$ are presented in figure 6(*b*), and in all cases look very similar, demonstrating an approximately 60 % decrease of the normalized volume-averaged kinetic dissipation rate in VC, compared to that in RBC.



https://doi.org/10.1017/jfm.2016.55 Published online by Cambridge University Press

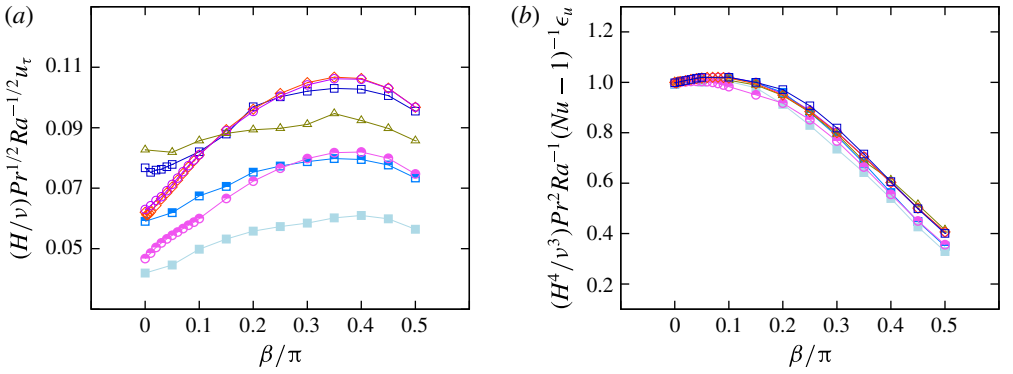



FIGURE 6. (*a*) Normalized friction velocity $(H/\nu)Pr^{1/2}Ra^{-1/2}u_\tau$, averaged in time and over the top and bottom plates in inclined convection in a cylinder of aspect ratio 1 as functions of the inclination angle $\beta$. (*b*) Normalized time- and volume-averaged kinetic dissipation rate $(H^4/\nu^3)Pr^2Ra^{-1}(Nu-1)^{-1}\epsilon_u$ in inclined convection in a cylinder of aspect ratio 1. $Pr = 0.1$ (triangles), $Pr = 1$ (squares), $Pr = 10$ (circles) and $Pr = 100$ (diamonds), and $Ra = 10^6$ (open symbols), $Ra = 10^7$ (half-filled symbols) and $Ra = 10^8$ (filled symbols).

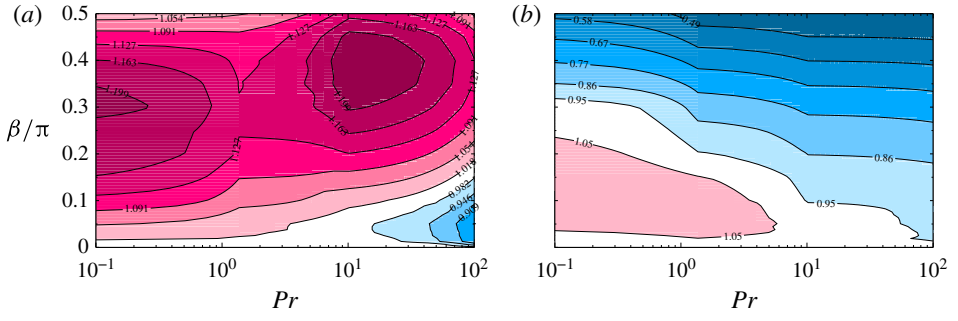



FIGURE 7. Phase diagrams for (*a*) $Nu/Nu(0)$ and (*b*) $Re/Re(0)$ in the ($Pr$, $\beta$) plane, showing the regions of a relative increase (pink) or decrease (blue) of the Nusselt and Reynolds numbers with respect to the RBC case ($\beta = 0$), as obtained in the DNS for $Ra = 10^6$.

## 3. Discussion

The conducted DNS show that the dependences on Nusselt number and Reynolds number in inclined convection are generally non-monotonic complicated functions of $Ra$ and $Pr$. Obviously, the geometry of the convection cell also influences these dependences. The results are summarized in figure 7, where phase diagrams for $Nu/Nu(0)$ and $Re/Re(0)$ are presented in the ($Pr$, $\beta$) plane. These diagrams show the regions of relative deviations of $Nu$ and $Re$ with the respect to the RBC case ($\beta = 0$), as obtained in the DNS.

In contrast to RBC ($\beta = 0$), in VC ($\beta = \pi/2$) the turbulent processes are much weaker, but the LSC is more coherent. In both limiting cases the heat transport is generally not as effective as in inclined convection, as obtained in all cases studied here ($Ra \leqslant 10^8$).

For small-Prandtl-number fluids, the velocity of the LSC (reflected in $Re$) starts to increase with $\beta$ even for a tiny tilt of the RBC cell, which leads to a more effective



https://doi.org/10.1017/jfm.2016.55 Published online by Cambridge University Press

heat transport. Thus, a felicitous combination of buoyancy and shear in inclined convection in fluids with $Pr \ll 1$ can lead to a significant increase of the mean heat flux, as obtained by Frick *et al.* (2015) and Kolesnichenko *et al.* (2015). The increase of $Nu$ compared to that in the RBC case is found to be larger for smaller $Pr$ and higher $Ra$.

In contrast to the small-$Pr$ fluid flows, for large $Pr$, a maximum of $Re(\beta)$ is obtained close to $\beta = 0$. The absolute increase of the LSC velocity due to the cell inclination is small, if any, and after a possible maximum the Reynolds number decreases gradually with increasing $\beta$. This drop in $Re$ is stronger for larger $Ra$. Thus, in large-$Pr$ fluids with high $Ra$, an increase of the heat transport due to an additional shear is not expected, and this is supported by a recent experiment by Guo *et al.* (2015), where a gradual decrease of $Nu$ with the cell inclination was obtained for $Pr \approx 6.7$ and $Ra \approx 4.4 \times 10^9$. We anticipate further, that for larger $Ra$ and $Pr > 1$, the decrease of $Nu(\beta)$ with increasing $\beta$ will be more pronounced for the following reasons. As our simulations show, for larger $\beta$, the onset of turbulence requires a larger $Ra$. Therefore, for the same $Ra$ the flow can already be in the fully turbulent regime in the case $\beta = 0$ (RBC) and still in the laminar or transitional regime in the case $\beta = \pi/2$ (VC). Since the scaling exponents in the $Nu$ versus $Ra$ scaling are generally larger for the turbulent regimes (Grossmann & Lohse 2000; Schlichting & Gersten 2000), the ratio of the Nusselt number at $\beta = \pi/2$ to the Nusselt number at $\beta = 0$ will gradually decrease with increasing $Ra$ in that range. The behaviour of $Nu(\beta)$ in large-$Pr$ fluids near $\beta = 0$ is quite complicated. The non-monotonicity of $Nu(\beta)$ in that region cannot be explained exclusively by a single- or multiple-roll structure of LSC, as non-monotonic dependences were obtained also in regions where a clear dominance of a single-roll global flow structure was observed.

The complicated behaviour of the $Nu$ versus $Ra$ dependence, with multiple extrema, in the studied range of $Ra$ and $Pr$ can be explained by the interaction of different transitions. Thus, for a fixed parameter $\beta = 0$ (RBC), the flow can vary from steady flow for small $Ra$ to turbulent flow for large $Ra$. Even when two parameters are fixed – namely, the Rayleigh number at a certain moderate value and $\beta = 0$ – the flow can be turbulent for small $Pr$ (Shishkina, Horn & Wagner 2013; Shishkina, Wagner & Horn 2014; Frick *et al.* 2015; Horn & Shishkina 2015) or non-turbulent (irregularly or periodically time-dependent) for large $Pr$ (Krishnamurti 1970; Bosbach, Weiss & Ahlers 2012; Horn *et al.* 2013; Horn & Shishkina 2014). When the parameter $\beta$ also varies, the situation becomes even more complicated, as with increasing $\beta$ the onset of turbulence moves to larger $Ra$. Moreover, with changing $\beta$, the symmetries of the flow change, influencing the $Nu(Ra, Pr, \beta)$ and $Re(Ra, Pr, \beta)$ dependences (see also Wei, Weiss & Ahlers (2015) on sharp transitions in RBC, caused by changes of flow symmetries).

For larger $Ra$, where the convection flows are turbulent for all $\beta$, the dependences should be simpler. As discussed, for large $Ra$ we expect a monotonic reduction of $Nu$ with increasing $\beta$ for large $Pr$, as in the experiments by Guo *et al.* (2015), and a single maximum for an intermediate value of $\beta$ in the $Nu$ versus $\beta$ dependence for the case of small $Pr$, as obtained in the measurements by Langebach & Haberstroh (2014), Frick *et al.* (2015), Kolesnichenko *et al.* (2015) and Vasilev *et al.* (2015). Further investigations of inclined convection in different fluids, both experimentally and numerically, for large and small $Pr$, are required for a better understanding of the mechanisms driving inclined convection and their $Re(\beta)$- and $Nu(\beta)$-dependences.



https://doi.org/10.1017/jfm.2016.55 Published online by Cambridge University Press

## Acknowledgements

O.S. is grateful to G. Ahlers, E. Bodenschatz, P. Frick, D. Lohse and S. Weiss for fruitful discussions. The authors acknowledge Leibniz Supercomputing Centre (LRZ) for providing computing time. O.S. acknowledges also financial support of the Deutsche Forschungsgemeinschaft (DFG) under the grant Sh405/4 (Heisenberg fellowship) and SFB 963/1, project A6.

## References

AHLERS, G., BROWN, E. & NIKOLAENKO, A. 2006 The search for slow transients, and the effect of imperfect vertical alignment, in turbulent Rayleigh–Bénard convection. *J. Fluid Mech.* **557**, 347–367.

AHLERS, G., GROSSMANN, S. & LOHSE, D. 2009 Heat transfer and large scale dynamics in turbulent Rayleigh–Bénard convection. *Rev. Mod. Phys.* **81**, 503–537.

BODENSCHATZ, E., PESCH, W. & AHLERS, G. 2000 Recent developments in Rayleigh–Bénard convection. *Annu. Rev. Fluid Mech.* **32**, 709–778.

BOSBACH, J., WEISS, S. & AHLERS, G. 2012 Plume fragmentation by bulk interactions in turbulent Rayleigh–Bénard convection. *Phys. Rev. Lett.* **108**, 054501.

BROWN, E. & AHLERS, G. 2006 Rotations and cessations of the large-scale circulation in turbulent Rayleigh–Bénard convection. *J. Fluid Mech.* **568**, 351–386.

CASTAING, B., GUNARATNE, G., HESLOT, F., KADANOFF, L., LIBCHABER, A., THOMAE, S., WU, X.-Z., ZALESKI, S. & ZANETTI, G. 1989 Scaling of hard thermal turbulence in Rayleigh–Bénard convection. *J. Fluid Mech.* **204**, 1–30.

CHILLÀ, F., RASTELLO, M., CHAUMAT, S. & CASTAING, B. 2004 Long relaxation times and tilt sensitivity in Rayleigh–Bénard turbulence. *Eur. Phys. J.* B **40** (2), 223–227.

CHILLÀ, F. & SCHUMACHER, J. 2012 New perspectives in turbulent Rayleigh–Bénard convection. *Eur. Phys. J.* E **35**, 58.

CILIBERTO, S., CIONI, S. & LAROCHE, C. 1996 Large-scale flow properties of turbulent thermal convection. *Phys. Rev.* E **54**, R5901–R5904.

CIONI, S., CILIBERTO, S. & SOMMERIA, J. 1997 Strongly turbulent Rayleigh–Bénard convection in mercury: comparison with results at moderate Prandtl number. *J. Fluid Mech.* **335**, 111–140.

FRICK, P., KHALILOV, R., KOLESNICHENKO, I., MAMYKIN, A., PAKHOLKOV, V., PAVLINOV, A. & ROGOZHKIN, S. A. 2015 Turbulent convective heat transfer in a long cylinder with liquid sodium. *Europhys. Lett.* **109**, 14002.

GROSSMANN, S. & LOHSE, D. 2000 Scaling in thermal convection: a unifying view. *J. Fluid Mech.* **407**, 27–56.

GUO, S.-X., ZHOU, S.-Q., CEN, X.-R., QU, L., LU, Y.-Z., SUN, L. & SHANG, X.-D. 2015 The effect of cell tilting on turbulent thermal convection in a rectangular cell. *J. Fluid Mech.* **762**, 273–287.

HORN, S. & SHISHKINA, O. 2014 Rotating non-Oberbeck–Boussinesq Rayleigh–Bénard convection in water. *Phys. Fluids* **26**, 055111.

HORN, S. & SHISHKINA, O. 2015 Toroidal and poloidal energy in rotating Rayleigh–Bénard convection. *J. Fluid Mech.* **762**, 232–255.

HORN, S., SHISHKINA, O. & WAGNER, C. 2013 On non-Oberbeck–Boussinesq effects in three-dimensional Rayleigh–Bénard convection in glycerol. *J. Fluid Mech.* **724**, 175–202.

KOLESNICHENKO, I. V., MAMYKIN, A. D., PAVLINOV, A. M., PAKHOLKOV, V. V., ROGOZHKIN, S. A., FRICK, P. G., KHALILOV, R. I. & SHEPELEV, S. F. 2015 Experimental study on free convection of sodium in a long cylinder. *Therm. Engng* **62**, 414–422.

KRISHNAMURTI, R. 1970 On the transition to turbulent convection. Part 2. The transition to time-dependent flow. *J. Fluid Mech.* **42**, 309–320.

LANGEBACH, R. & HABERSTROH, C. 2014 Natural convection in inclined pipes – a new correlation for heat transfer estimations. In *AIP Conference Proceedings*, vol. 1573, pp. 1504–1511.



https://doi.org/10.1017/jfm.2016.55 Published online by Cambridge University Press

LOHSE, D. & XIA, K.-Q. 2010 Small-scale properties of turbulent Rayleigh–Bénard convection. *Annu. Rev. Fluid Mech.* **42**, 335–364.

NG, C. S., OOI, A., LOHSE, D. & CHUNG, D. 2015 Vertical natural convection: application of the unifying theory of thermal convection. *J. Fluid Mech.* **764**, 349–361.

ROCHE, P.-E., GAUTHIER, F., KAISER, R. & SALORT, J. 2010 On the triggering of the ultimate regime of convection. *New J. Phys.* **12** (8), 085014.

SCHLICHTING, H. & GERSTEN, K. 2000 *Boundary-Layer Theory*, 8th edn. Springer.

SHISHKINA, O., HORN, S. & WAGNER, S. 2013 Falkner–Skan boundary layer approximation in Rayleigh–Bénard convection. *J. Fluid Mech.* **730**, 442–463.

SHISHKINA, O., HORN, S., WAGNER, S. & CHING, E. S. C. 2015 Thermal boundary layer equation for turbulent Rayleigh–Bénard convection. *Phys. Rev. Lett.* **114**, 114302.

SHISHKINA, O., STEVENS, R. J. A. M., GROSSMANN, S. & LOHSE, D. 2010 Boundary layer structure in turbulent thermal convection and its consequences for the required numerical resolution. *New J. Phys.* **12**, 075022.

SHISHKINA, O. & WAGNER, S. 2016 Prandtl-number dependence of heat transport in laminar horizontal convection. *Phys. Rev. Lett.* **116**, 024302.

SHISHKINA, O., WAGNER, S. & HORN, S. 2014 Influence of the angle between the wind and the isothermal surfaces on the boundary layer structures in turbulent thermal convection. *Phys. Rev.* E **89**, 033014.

SIGGIA, E. 1994 High Rayleigh number convection. *Annu. Rev. Fluid Mech.* **26**, 137–168.

SUN, C., XI, H.-D. & XIA, K.-Q. 2005 Azimuthal symmetry, flow dynamics, and heat transport in turbulent thermal convection in a cylinder with an aspect ratio of 0.5. *Phys. Rev. Lett.* **95**, 074502.

VASILEV, A. YU., KOLESNICHENKO, I. V., MAMYKIN, A. D., FRICK, P. G., KHALILOV, R. I., ROGOZHKIN, S. A. & PAKHOLKOV, V. V. 2015 Turbulent convective heat transfer in an inclined tube filled with sodium. *Tech. Phys.* **60**, 1063–7842.

WEI, P., WEISS, S. & AHLERS, G. 2015 Multiple transitions in rotating turbulent Rayleigh–Bénard convection. *Phys. Rev. Lett.* **114**, 114506.

WEI, P. & XIA, K.-Q. 2013 Viscous boundary layer properties in turbulent thermal convection in a cylindrical cell: the effect of cell tilting. *J. Fluid Mech.* **720**, 140–168.

WEISS, S. & AHLERS, G. 2013 Effect of tilting on turbulent convection: cylindrical samples with aspect ratio $\gamma = 0.50$. *J. Fluid Mech.* **715**, 314–334.

https://doi.org/10.1017/jfm.2016.55 Published online by Cambridge University Press